*Acta Oceanol. Sin.*, 2011, Vol. 30, No. 4, P. 53-59
DOI: 10.1007/s13131-011-0133-4
http://www.hyxb.org.cn
E-mail: hyxbe@263.net

# The color reflectance of marine-terrigenous deposits in LZ908 borehole in south coastal plain of the Laizhou Bay

ZHAO Na[1,2,3], XU Xingyong[3]*, YU Hongjun[3], YAO Jing[3], SU Qiao[3], PENG Shuzhen[4]

[1] Yantai Institute of Coastal Zone Research, Chinese Academy of Sciences, Yantai 264003, China

[2] Graduate University of Chinese Academy of Sciences, Beijing 100049, China

[3] the First Institute of Oceanography, State Oceanic Administration People's Republic of China, Qingdao 266061, China

[4] Taishan University, Taian 271021, China

Received 19 September 2010; accepted 27 January 2011



**Abstract**
Color measuring is characterized by high resolution, high efficiency, and low cost. The application becomes increasingly common for tracing sediment sources and climate variation. Borehole LZ908 in the south coastal plain of the Laizhou Bay in northeast China, was used, of which the top 54 m containing all marine facies was focused, to test the feasibility of colorimetry as a climate indicator using visible light reflectance spectra and L*a*b* measurement results. The results show a good correction between lightness and calcium carbonate content in marine-terrigenous deposits; therefore, these deposits can be used as a proxy to study climate changes. Factor-analysis on the first derivative values of the raw visible light reflectance spectra produced three principal factors corresponding to goethite, organic matter, and hematite. Down hole variations in the three factor scores, lightness, calcium carbonate content, and grain size were quite consistent. Moreover, high lightness and low factor scores in goethite, hematite, and organics indicated glacial regression deposits, while low lightness and high factor scores in goethite, hematite, and organics indicated interglacial transgression deposits.

**Key words:** coastal plain, the Laizhou Bay, visible light reflectance, factor analysis, L*a*b*, lightness

## 1 Introduction

Sediment color is a readily observable physical property of internal components as reflected radiation in the visible region of electromagnetic spectrum (400–700 nm) (Balsam et al., 1997).

In geological studies, sediment color is usually determined by comparing it by human-eyes against a standard color chart, such as the Munsell color chart. However, as a qualitative system, the result varies individually in operator; data recorded in this system cannot be easily manipulated mathematically and may vary in quality as condition changes in observer and/or observation (Giosan et al., 2002). Alternative to the Munsell system is the CIE/L*a*b* system defined by the Commission International on Illumination (CIE, 1976). It has been widely used for its specifying illuminant and quantifying color descriptors (Balsam et al., 1999). The L* value, a lightness parameter, is scaled 0–100 from black to white and is approximately equivalent to gray-scale reflectance (Chapman and Shackleton, 1998). In most cases, L* is interpreted as variation in carbonate content (Balsam et al., 1999), which has been shown as an important climate indicator for high-resolution sediment studies (Ji et al., 2001; Porter, 2000). Both a* and b* are chromaticity parameters: a* for red (positive values) to green (negative values) hues and b* for yellow (positive values) to blue (negative values) hues (Wang et al., 2003). Konica Minolta machines are commonly used for L*a*b* measurement. They are designed to scan the light reflected from the surface of an object and record the spectrum relative to a white standard (e.g., barium sulfate) (Balsam et al., 1998). Many studies have

Foundation item: The National Natural Science Foundation of China under contract No. 40602018; the Chinese Offshore Investigation and Assessment ("908" Program) under contract No. 908-01-ZH2; the Marine Welfare Research Project under contract No. 200805063.
*Corresponding author, E-mail: xuxingyong@fio.org.cn

shown that components of marine sediment have distinctive spectral signatures, and visible light (VIS) reflectance spectra have been used to indentify iron oxide and oxyhydroxide minerals, clay minerals, and sediment organic content, etc (Balsam et al., 1997; Balsam and Wolhart, 1993; Balsam and Deaton, 1991; Deaton and Balsam, 1991).

However, studies on sediment color have been done for deep-sea sediments (Balsam et al., 1999; Balsam et al., 1998), loess-paleosol sequences (Balsam et al., 2004; Chen et al., 2002; Ji et al., 2001; Porter, 2000), shelf sediment (Wang et al., 2007; Wang et al., 2006), and lake sediment (Wu and Li, 2004). This study is focused on marine-terrigenous deposits of a coastal plain, a transitional zone between land and sea, and also an intersectional zone among hydrosphere, lithosphere, biosphere, and atmosphere, featuring deposits of complicated sources under dynamic conditions.

The studied drilling core LZ908 (37°09′N, 118°58′E), 101.3 m long, was taken in 2007 in south coastal plain of the Laizhou Bay, the Bohai Sea of China (Fig. 1). The place of the core was near the central basin of the Bohai Sea and the north Huanghai Sea (Yellow Sea) to the east. To the west and the south are surrounded by the modern Huanghe River (Yellow River) delta and the Quaternary alluvial-marine plain with many south-flowing rivers originated from central mountains in the Shandong Peninsula.

The upper about 54 m of the borehole was sandy and silty intercalated by several clay layers rich in shell fragments, and was considered as marine-terrigenous deposits (Yao et al., 2010), which is focused in this paper. The lower part was mainly silty deposit with abundant calcareous nodules. Previous researches show that, since the Late Pleistocene, the Laizhou Bay has developed several transgression horizons, recording fluctuations in sea level and shoreline changing in history (Zhao, 1996; Han and Meng, 1986).

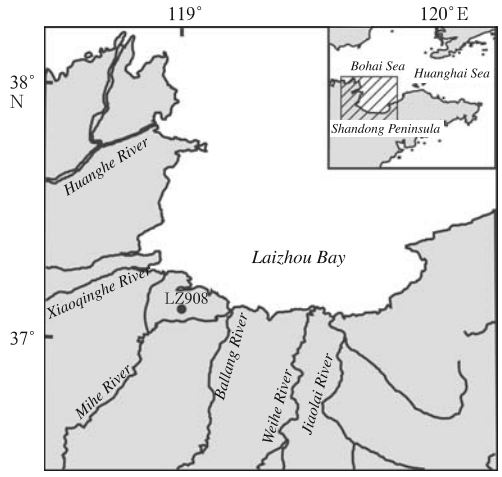


**Fig.1.** Location of the core.

## 2 Materials and methods

### 2.1 *Color measurement*

Color measurements were performed individually by a Minolta CM-2002 spectrophotometer and a Minolta CR400/410 colorimeter. Both machines selected L*a*b* as color space, set 8 mm aperture, and chose SCE (specular component excluded) to free the impact of glassy cover on sediment surface.

Minolta CM-2002 was used for fresh surfaces of core for instant in-situ measurement once the core was opened. Upon opening, the core was covered with polyethylene film (clean plastic wrap) to prevent water loss and color change due to oxidation (Chapman and Shackleton, 1998), avoid contamination from the spectrophotometer (Debret et al., 2006), and protect the instrument from damage by water and wet sediment (Balsam et al., 1997). Measurements were taken directly in 1 cm interval at core surface through the plastic food wrap. Diffused reflectance spectra values at 31 wavelengths (400–700 nm at 10 nm intervals) and L*a*b* values of each measurement were stored on the memory card of the Minolta device.

Afterwards, samples were collected at 10 cm interval from the core for another L*a*b* measurement by a Minolta CR400/410 colorimeter. Collected samples were air dried at room temperature and then were ground. Measurements were taken directly on ground samples.

L*a*b* values measured by the Minolta CR400/410 presented a good relationship with calcium carbonate content and grain size, which will be discussed later. In addition, we had to use diffused reflectance spectra values from the Minolta CM–2002 because they were unavailable from the Minolta CR400/410 colorimeter.

### 2.2 *Calcium carbonate content measurement*

Mass percentage of calcium carbonate was determined in volumetry (GB/T13909–92). Samples were collected at 10 cm intervals downcore. Approximately 0.1 g for each sample was placed in a 100 ml triangular flask and was humidified with a drop of water. Add 10 ml of 0.1 mol/dm$^3$ HCl into the container, shake

up, and keep slightly boiling for 3 min. Move the container into water-bath at 70–80°C for 10–20 min, then remove it after carbonate was totally dissolved. Add 2–3 drops of phenolphthalein indicator when mixture cooled, and titrate it with 0.1 mol/dm$^3$ NaOH standard solution. Meanwhile, a blank test was preformed. The following formula is used to calculate the calcium carbonate content (%):

$$\omega_{(\mathrm{CaCO_3})} = \frac{(V_0 - V_1)c_{(\mathrm{NaOH})} \times F}{m} \times 100.$$

Where $c_{(\mathrm{NaOH})}$ is the concentration (mol/dm$^3$) of NaOH standard solution; $V_1$ is the volume (ml) of consumed NaOH used by each sample; $V_0$ is the volume (ml) of consumed NaOH used by the blank test; $m$ is the mass (g) of each sample; $F$ is $50.04\times10^{-3}$, be equal to the mass (g) of $CaCO_3$ which consumed 1 ml of 1 mol/dm$^3$ NaOH.

### 2.3 *Grain size measurement*

Samples were collected at 2 cm intervals down core for grain size measurements by Malvern's Mastersizer–2000 with a measurement range 0.02–2 000 $\mu$m. The error was within ±3% as per parallel measurement.

## 3 Results and discussion

### 3.1 *Diffuse reflectance spectral*

VIS reflectance spectra measured were factor-analyzed on the first derivative values of raw spectra data using wavelength as variables. A factor analysis is a rapid and common method used to extract information that is compositionally unique (Giosan et al., 2002; Ji et al., 2001; Balsam et al., 1997; Balsam and Wolhart, 1993). The previous work has shown that the maximum compositional information can be extracted from spectral data by factor analyzing the first-derivative values (Balsam and Deaton, 1991). We assembled the first-derivative data from upper 54 m of the core into a matrix of 3 799 samples (rows) by 30 first-derivative values (columns: 405 nm to 695 nm at 10 nm intervals). The matrix was analyzed with SPSS (Version 15) using a principal-factor method. R-mode factor analysis was used to group the first-derivative variables into factors (Balsam et al., 1997) and varimax rotation was employed to maximize the variance among variables (Balsam and Wolhart, 1993). The first three principal factors were produced by factor analysis explained about 94.4% of the cumulative variance (Table 1). Using the three factors, all the wavelengths were explained in communality greater than 0.9.

The challenge of the factor-analysis on VIS spectral data is to relate a factor to a particular sediment component (Balsam and Wolhart, 1993). Ideally, it should be possible to interpret factors by comparing factor loadings to the first derivative curve for various sediment components (Balsam and Wolhart, 1993).

The curve of loading for Factor 1 covers much of the variance so that it is difficult to relate it to a particular sediment component (Fig. 2). Balsam and Deaton (1991) noted that samples of high-score should characterize that factor. We plot first-derivative curves for sample of high-score (Fig. 3). The curve has two distinct peaks: one is at 435 nm; the other is in 515–555 nm, which is interpreted as goethite domination because goethite has a principal peak at 535 nm and a secondary one at 435 nm (Deaton and Balsam, 1991). The broadness of the peak from 515–555 nm suggests some hematites.

**Table 1.** Total variance explained

| Component | Initial eigenvalues | | | Extraction sums of squared loadings | | |
|---|---|---|---|---|---|---|
| | Total | Variance(%) | Cumulative(%) | Total | Variance(%) | Cumulative(%) |
| 1 | 16.450 | 54.833 | 54.833 | 16.450 | 54.833 | 54.833 |
| 2 | 10.126 | 33.753 | 88.587 | 10.126 | 33.753 | 88.587 |
| 3 | 1.732 | 5.772 | 94.359 | 1.732 | 5.772 | 94.359 |
| 4 | 1.031 | 3.438 | 97.797 | | | |
| 5 | 0.207 | 0.690 | 98.487 | | | |
| 6 | 0.127 | 0.423 | 98.910 | | | |

Factor 2 (Fig. 2) appears to be organic origin causing absorption increase at the violet end of the spectrum and reflectance one at the red end of the spectrum (Balsam and Deaton, 1991). In a coastal plain, marine-terrigenous deposits formed during an interglacial transgression usually contain more organisms, and less during a glacial regression.

Factor 3 is a unimodal factor featuring a peak at

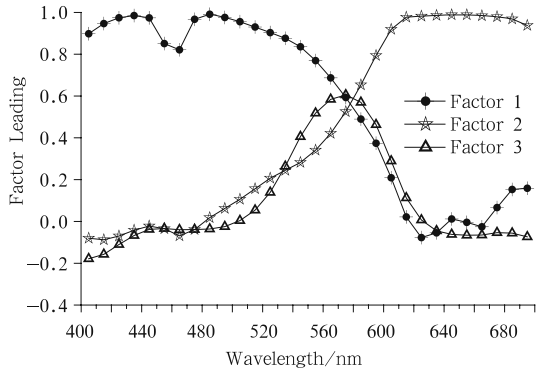


**Fig.2.** Curves of factor loadings as a function of wavelength.

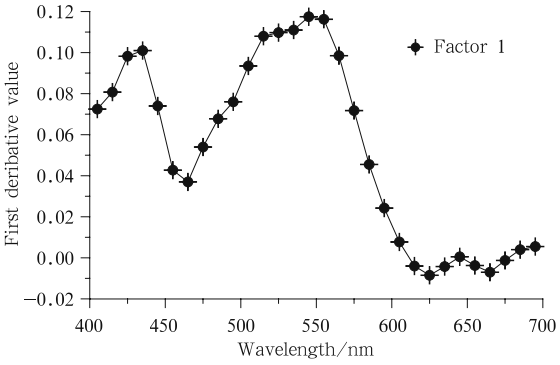


**Fig.3.** First-derivative curves for samples with high scores for Factor 1.

555 nm in the first derivative situated between 555 and 575 nm, which is probably hematite related, which is characterized by the unique peak. The exact place of the peak varies with hematite content (Barranco et al., 1989).

### 3.2 *Lightness and calcium carbonate content*

L* or lightness, varying from 40.4 to 77.7 (Fig. 4), has a close relationship with calcium carbonate content (Table 2). Curves of the trends and the peaks are generally consistent (Fig. 4). It is reasonable to use lightness as a proxy for calcium carbonate content in marine-terrigenous deposits in this case.

**Table 2.** Correlation among carbonate content and two measurements of a*, b* and L*

| | a* | b* | L* | $c(CaCO_3)$ |
|---|---|---|---|---|
| a* | 1 | | | |
| b* | 0.698** | 1 | | |
| L* | –0.213** | –0.099 | 1 | |
| $c(CaCO_3)$ | –0.256** | –0.392** | 0.503** | 1 |

Notes: **indicates that correlation is significant at the 0.01 level (2-tailed). $n$=376.

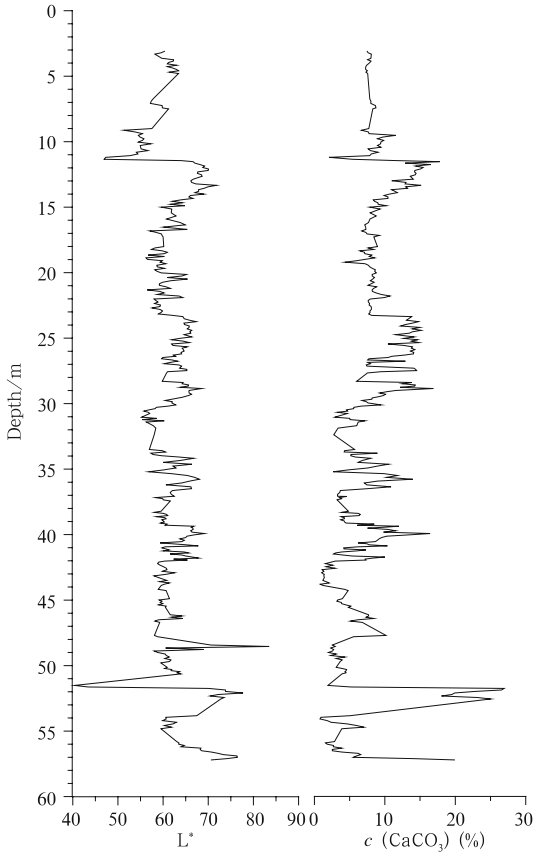


**Fig.4.** Down core curves of L* and calcium carbonate content.

In this study, lightness values reduced when calcium carbonate content decreased. However, their scatter plot seems interesting (Fig. 5). Generally, as calcium carbonate content decreases, lightness falls down; and this trend is broken when calcium carbonate content falls within 5%. The dots fluctuate greatly around 60.00 (Fig. 5).

Such a phenomenon may attribute to the non-carbonate fraction in the sediments. When calcium carbonate content is less than 5%, the lightness reflects mainly the non-carbonate fraction. Two situations should be considered. Number one, when calcium carbonate content is less than 5%, some light components may appear or increase. Balsam et al. (1999) mentioned that if non-carbonate fraction is mainly light components, L* would show little change as carbonate content decreases. Number two, some dark components may be contained (such as organic matters), disappear, or decrease. Reduction in calcium carbonate content would slow down the decrease of lightness, causing fluctuation of lightness value.

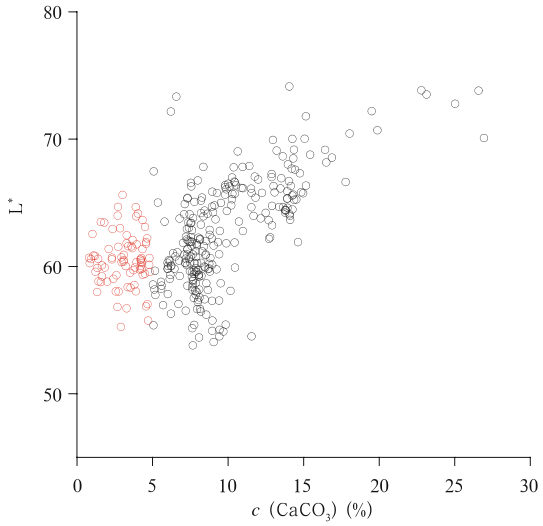


**Fig.5.** Variations in L* as a function of calcium carbonate content. Red circles indicate calcium carbonate content is less than 5%. Black circles indicate calcium carbonate content is more than 5%.

### 3.3 *Chromaticity*

a* values changing from –0.28 to 5.5 are almost positive, while b* values fluctuating from 7.36 to 34.02 are all positive. a* and b* have a superior positive relationship. Their down hole values present an opposite tendency against L* and calcium carbonate content (Fig. 6). The correlation coefficient is shown in Table 2.

Similar to the four principal factors, red hue may be attributed to hematite. Higher the hematite content is, redder the sediment is, and the greater a* would be as well. The yellow hue may result from goethite. The higher the goethite content is, the yellower sediment is, and then the bigger b* is. Hematite tends to form in semi humid, semi arid, or even arid climates, while goethite does so in humid and temperate areas (Balsam and Wolhart, 1993). In this case, high a* and b* values suggest that sediments formed in seasonal conditions alternating between hot-dry and warm-wet (Wang et al., 2009).

### 3.4 *Downhole variations in factors*

Since the Late Pleistocene, alternation of glacial and interglacial periods in the Bohai Sea area resulted in the shift between transgression and regression, and consequently the marine-terrigenous deposits are formed in the coastal plain. Generally, sediments formed in glacial periods contain more calcium carbonate, consist of more silts, and more eolian in origin. Sediments in interglacial periods include less calcium carbonate and consist of more sands (Zhao, 1996). In addition, as mentioned above, marine deposits have more organics, goethite, and hematite than terrigenous deposits do.

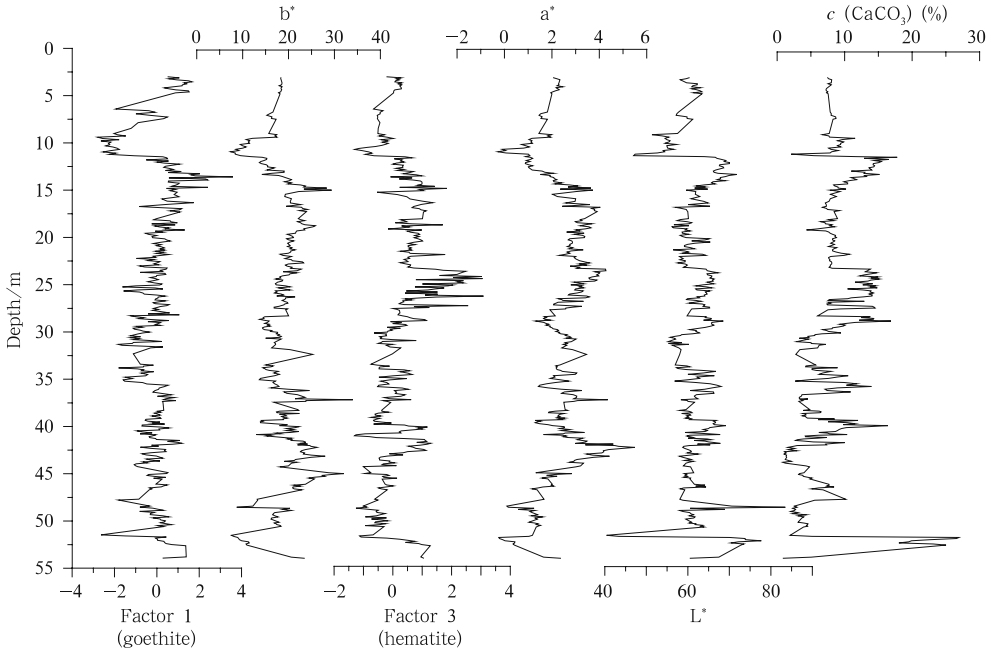


**Fig.6.** Down core variations in color indices, $CaCO_3$, and factor scores for goethite and hematite.

Factor scoring that indicates the importance of each factor of a study system, provides a spatial-temporal record of changes in a factor. If a factor is related to a single or combined components of the sediments, factor-scoring will present a semi quantitative estimate of changes in those components (Balsam et al., 1997). As shown in Fig. 7, down hole variations are ascribed by three principal factors. By comparing the factors with curves of lightness, calcium carbonate content, and grain size, a general trend of the climate is indicated, which will be discussed as follows.

In Core LZ908, two paleoclimate indicators, calcium carbonate content and grain size, were well correlated: positive for clay (0–4 $\mu$m) and silt (4–63 $\mu$m), but negatively for sand (>63 $\mu$m) (Fig. 7, Table 3). In this case, sediments of high lightness values corresponded to high calcium carbonate content, and were mainly terrigenous, indicative of glacial regime, while those of low lightness values reflected low calcium carbonate content and were more marine, indicative of interglacial regime. This is supported by a previous research (Yao et al., 2010) in which the transgression strata of Core LZ908 were confirmed by abundant and diversified foraminifers. Of Core LZ908, layers rich in genera of coastal to medium shallow marine species were those of low lightness values and high factor scores in goethite, hematite, and organics components, reflecting interglacial transgression feature, while those of layers poor in genera of coastal to medium shallow marine species were those of high lightness values and low factor scores in goethite, hematite, and organism components, indicating glacial regression feature.

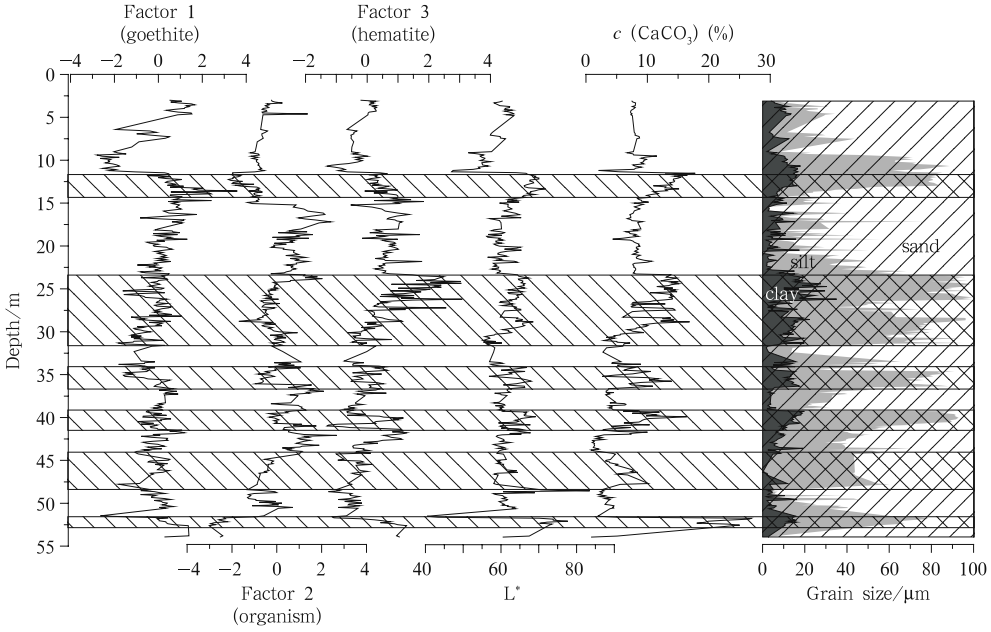


**Fig.7.** Variations in factor scores.

**Table 3.** Correlation of lightness, calcium carbonate content, and grain size

| | Clay | Silt | Sand |
|---|---|---|---|
| $L_2^*$ | 0. 243** | 0.166** | –0.194** |
| $c(CaCO_3)$ | 0.368** | 0.405** | –0.417** |

Notes:**indicates that correlation is significant at 0.01 level (2-tailed). $n$=376.

## 4 Conclusions

(1) Three principal factors were explained by goethite, organism, and hematite, respectively, and were revealed by analyzing the first derivative of raw spectral curve in Core LZ908 samples from the south coastal plain of the Laizhou Bay, and they solved about 94.4% of the total cumulative variance.

(2) Lightness showed a relationship with calcium carbonate content ($r$=0.503, $n$=376). As calcium carbonate content is less than 5%, the lightness values do not decrease as calcium carbonate content decreases, but fluctuate around 60.00. Such a phenomenon may attribute to non-carbonate components of sediments, for example, organism.

(3) In marine-terrigenous deposits in the coastal plain of the Laizhou Bay, glacial regression deposits presented high lightness values and low factor scores. Contrarily, interglacial transgression sediments showed low lightness values and high factor scores.

***Acknowledgements***

The authors are grateful to Dr. Wang Kunshan from the First Institute of Oceanography, the State Oceanic Administration and Zhu Lijun from Shanxi Normal University for color measurements. Thanks also go to Yi Liang, Jiang Xingyu, and Xu Yuanqin for decimating samples.

## References

Balsam W L, Damuth J E, Schneider R R. 1997. Comparison of shipboard vs. shore-based spectral data from Amazon Fan cores: implications for interpreting sediment composition. Proceedings of the Ocean Drilling Program, Scientific Results, 155: 193–215

Balsam W L, Deaton B C. 1991. Sediment dispersal in the Atlantic Ocean: evaluation by visible light spectra. Journal of Aquatic Research, 4: 411–447

Balsam W L, Deaton B C, Damuth J E. 1998. The effects of water content on diffuse reflectance spectrophotometry studies of deep-sea sediment cores. Marine Geology, 149: 177–189

Balsam W L, Deaton B C, Damuth J E. 1999. Evaluating optical lightness as a proxy for carbonate content in marine sediment cores. Marine Geology, 161: 141–153

Balsam W L, Ji J F, Chen J. 2004. Climatic interpretation of the Luochuan and Lingtai loess sections, China, based on changing iron oxide mineralogy and magnetic susceptibility. Earth and Planetary Science Letters, 223: 335–348

Balsam W L, Wolhart R J. 1993. Sediment dispersal in the Argenine Basin: evidence from visible light spectra. ELiang, e Oceanic Administration Deep-Sea Research II, 40(4/5): 1001–1031

Barranco F T Jr, Balsam W L, Deaton B C. 1989. Quantitative reassessment of brick red lutites: evidence from reflectance spectrophotometry. Marine Geology, 89(3–4): 299–314

Chapman M R, Shackleton N J. 1998. What level of resolution is attainable in a deep-sea core? Results of a spectrophotometer study. Paleoceanography, 13(4): 311–315

Chen Jun, Ji Junfeng Balsam W L, et al. 2002. Characterization of the Chinese loess-paleosol stratigraphy by whiteness measurement. Palaeogeography, Palaeoclimatology, Palaeoecology, 183: 287–297

Deaton B C, Balsam W L. 1991. Visible spectroscopy–A rapid method for determining hematite and goethite concentration in geological materials. Journal of Sedimentary Petrology, 61: 628–632

Debret M, Desmet M, Balsam W L, et al. 2006. Spectrophotometer analysis of Holocene sediments from an anoxic fjord: Saanich Inlet, British Columbia, Canada. Marine Geology, 229: 15–28

Giosan L, Flood R D, Aller R C. 2002. Paleoceanographic significance of sediment color on western North Atlantic drifts: I. Origin of color. Marine Geology, 189: 25–41

Han Yousong, Meng Guanglan. 1986. Sea Level Change in China (in Chinese). Beijing: China Ocean Press, 98–104

Ji Jungfeng, Balsam W L, Chen Jun. 2001. Mineralogic and climatic interpretations of the Luochuan loess section (China) based on diffuse reflectance spectrophotometry. Quatenary Research, 56: 23–30

Porter S C. 2000. High-resolution paleoclimatic information from Chinese eolian sediments based on grayscale intensity profiles. Quaternary Research, 53: 70–77

Wang Hong, Hughes R E, Steele J D, et al. 2003. Correlation of climate cycles in middle Mississippi Valley loess and Greenland ice. Geology, 31(2): 179–182

Wang Hong, Lundstrom C C, Zhang Zhaofeng, et al. 2009. A Mid-Late Quaternary loess-paleosol record in Simmons Farm in southern Illinois, USA. Quaternary Science Reviews, 28: 93–106

Wang Kunshan, Shi Xuefa, Cheng Zhenbo, et al. 2007. Analysis of affecting factors for reflectance spectra of sediments from the central shelf area of the southern Yellow Sea. Advances in Marine Science (in Chinese), 25(1): 46–53

Wang Kunshan, Shi Xuefa, Wang Guoqing. 2006. A preliminary study on the sediment color reflectance in the southern Yellow Sea shelf area. Advances in Marine Science (in Chinese), 24(1): 30–38

Wu Yanhong, Li Shijie. 2004. Significance of lake sediment color for short time scale climate variation. Advances in Earth Science (in Chinese), 19(5): 789–792

Yao Jing, Yu Hongjun, Xu Xingyong, et al. 2010. Marine transgression record in the marine-terrigenous facies deposits on south coast of Laizhou Bay. Inshore and Coastal Geological Hazards (in Chinese). Beijing: China Ocean Press, 49–56

Zhao Songling. 1996. Shelf Desertization (in Chinese). Beijing: China Ocean Press, 178–183, 164–166